Heat capacity evidence for conventional superconductivity in the type-II Dirac semimetal $PdTe_2$

Amit and Yogesh Singh
Department of Physical Sciences, Indian Institute of Science Education and Research (IISER) Mohali, Knowledge City, Sector 81, Mohali 140306, India

(Received 22 December 2017; revised manuscript received 6 February 2018; published 21 February 2018)

We use electrical transport, magnetoresistance, and heat capacity measurements on high quality single crystals of the recently discovered superconducting type-II Dirac semimetal $PdTe_2$, to probe the nature of its superconducting phase. The magnitude of the electronic heat-capacity anomaly at T_c, the low temperature exponential T dependence of the heat capacity, the linear H dependence of the $T = 0$ electronic Sommerfeld coefficient, and a conventional $H - T$ phase diagram establish that the superconductivity in $PdTe_2$ is conventional in nature despite the presence of a topologically nontrivial Fermi surface band, which contributes to the electrical conduction.

DOI: 10.1103/PhysRevB.97.054515

I. INTRODUCTION

Topological superconductors (TSCs) have been the focus of intense recent research [1]. This is in part due to the possibility that these materials may host Majorana fermion excitations [2,3] which, in addition to being of fundamental interest, can also be used in fault-tolerant Quantum computation. Additionally, several predictions for TSC suggest unconventional superconducting properties like point or line nodes in the gap structure, unconventional pairing, mixed order parameters, and the possibility of an Fulde-Ferrell-Larkin-Ovchinnikov (FFLO) state [1,4–7]. To stabilize topological superconductivity (TSC), various routes have been pursued. For example, doping [8–15] or pressurizing [16] a parent topological material, studying chiral spin-triplet superconductors [17], making heterostructures of a semiconductor with a conventional superconductor [18,19], or a topological material with a conventional superconductor [20,21]. Another exciting new avenue has opened up in which superconductivity has been shown to emerge in nanoscale point contacts between topological materials and normal metals [22–24].

In all these routes, superconductivity is induced by some tuning like doping, pressure, proximity, or confinement. It would be ideal to look for a system in which topological band structure and superconductivity emerge naturally and to then demonstrate the topological character of the superconductivity.

Recently, a new family of transition-metal dichalcogenide materials AX_2 (A = Pt, Pd, X = Te, Se) have been shown to be type-II Dirac materials where the electronic band structure consists of a tilted Dirac cone [25–28]. This follows the discovery of type-II Weyl materials [29–35]. Both the type-II Weyl and Dirac fermions observed in the above materials break Lorentz invariance and are therefore fundamentally different quasiparticles compared to the normal type-I Dirac and Weyl fermions discovered earlier. The study of the properties of these type-II topological materials are therefore of immense fundamental interest and could lead to important technological applications. How conventional or fairly well-understood states of matter like magnetism or superconductivity emerge in materials with topological band structures has been an emerging frontier area of research. In this context, $PdTe_2$ is especially important since it is known to also host a superconducting state below the critical temperature $T_c \approx 1.7$ K [36,37]. While there are now several theoretical studies on TSC in type-I topological materials [1,4–6], to our knowledge there is only one theoretical study of superconductivity in type-II topological materials [7]. That study showed that unconventional superconductivity with a nodal gap structure will emerge if the superconductivity in $PdTe_2$ involves electrons in the tilted topological band [7]. TSC in $PdTe_2$ is thus an exciting possibility, which needs to be carefully examined.

In this paper, we report electrical transport, magnetotransport, and heat capacity C measurements on high quality single crystals of the superconducting type-II Dirac semimetal $PdTe_2$ to explore the possible unconventional (topological) nature of the superconducting state. We confirm superconductivity with a critical temperature $T_c \approx 1.7$ K using electrical transport measurements. From recent de Haas-Van Alphen (dHvA) oscillations in magnetization measurements, we have shown that four bands contribute to the transport, including a band with a nontrivial Berry phase [38]. This raises the enticing possibility of TSC in $PdTe_2$. Our heat capacity measurements demonstrate bulk superconductivity below $T_c \approx 1.7$ K. The size of the superconducting anomaly in the heat capacity ΔC at T_c is estimated to be $\Delta C/\gamma T c \approx 1.52$, which is close to the value 1.43 expected for a conventional weak-coupling single-gap BCS superconductor. The $C(T)$ at low temperature shows an exponential T dependence suggesting a fully gapped superconducting state. Additionally, the $C(T)$ data in various applied magnetic fields H is used to construct an H-T phase diagram, which also shows conventional behavior. Finally, the $T = 0$ electronic Sommerfeld coefficient shows a linear H dependence ruling out nodes in the superconducting gap. Thus, our measurements strongly indicate that the superconductivity in $PdTe_2$ is conventional in nature despite the presence of topologically nontrivial electrons contributing to the transport.

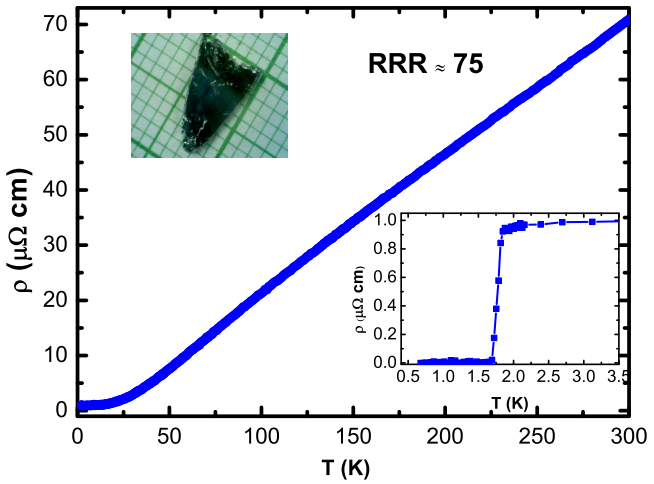

FIG. 1. Electrical resistivity ρ versus T for $PdTe_2$ measured in zero applied magnetic field with a current $I = 0.5$ mA applied in the crystallographic ab plane. The top inset shows an optical image of a $PdTe_2$ crystal placed on a millimeter grid. The bottom inset shows the $\rho(T)$ data below 3 K to highlight the superconducting transition with $T_c \approx 1.75$ K.

II. EXPERIMENTAL

Single crystals of $PdTe_2$ were synthesized using a modified Bridgeman method. The starting elements, Pd powder (99.99% purity) and Te shots (99.9999%), were weighed in the atomic ratio 1 : 2.2 and sealed in an evacuated quartz tube. The 10% extra Te was taken to compensate for Te loss due to its high vapor pressure. For crystal growth, the tube with the starting materials was heated to 790 °C in 15 h, kept there for 48 h, and then slowly cooled to 500 °C over seven days. The tube was then annealed at 500 °C for five days before cooling naturally to room temperature. The shiny crystals of millimeter size thus obtained could be cleaved easily from the as-grown boule. A typical crystal is shown on a millimeter grid in the inset of Fig. 1. The chemical composition of crystals was verified by energy dispersive spectroscopy (EDS) on a JEOL SEM. The ratio given by EDS between Pd and Te was 1:1.99, showing the stoichiometric ratio of the compound. A few crystals were crushed into powder for x-ray diffraction measurements. The powder x-ray diffraction pattern confirms the phase purity of $PdTe_2$, well crystallized in the CdI_2-type structure with the $P3m1$(164) space group.

The electrical transport and heat capacity down to 0.4 K were measured using the He3 option of a quantum-design physical property measurement system (QD-PPMS).

III. ELECTRICAL TRANSPORT

Figure 1 shows the electrical resistivity ρ versus temperature T measured in zero magnetic field with a current $I = 0.5$ mA applied within the crystallographic ab plane. The $\rho(T)$ shows metallic behavior with $\rho(300\ \text{K}) \approx 70\,\mu\Omega$ cm and $\rho(2\ \text{K}) \approx 0.94\,\mu\Omega$ cm, giving a residual resistivity ratio $RRR \approx 75$. This RRR is larger than reported earlier, indicating that the $PdTe_2$ crystals are of high quality. The lower inset in Fig. 1 shows the $\rho(T)$ data below $T = 3$ K and the abrupt drop to zero resistance below $T_c = 1.75$ K confirms the superconductivity in $PdTe_2$.

We have recently reported [38] observation of quantum oscillations in the magnetization measurements on $PdTe_2$ crystals below $T = 20$ K, again suggesting the high quality of the samples. For magnetic field applied perpendicular to the c axis, we observed a single frequency at 439 T in the fast Fourier transform of the dHvA data. The Berry phase for this band was estimated to be nontrivial, suggesting its topological nature. Additionally, three other frequencies were observed for $H||c$-axis. Thus there are multiple electronic bands including a topological band contributing to the transport, and it is unclear from just transport measurements whether the observed superconductivity itself has any unconventional topological character.

IV. HEAT CAPACITY

We have therefore used heat capacity measurements to address the nature of superconductivity in $PdTe_2$. Figure 2(a) shows the heat capacity C versus temperature T data for $PdTe_2$ between $T = 0.4$ and 3 K measured in $H = 0$ and $H = 500$ Oe magnetic field. A sharp anomaly at $T_c = 1.72$ K in the $H = 0$ data indicates that the superconductivity in $PdTe_2$ is bulk in nature. No anomaly is observed down to the lowest temperatures measured in $H = 500$ Oe, suggesting that the superconductivity has been completely suppressed. This is confirmed by our heat capacity data in various magnetic fields, which will be presented later. The $H = 500$ Oe data was treated as the normal state data and was fit to the expression $C = \gamma T + \beta T^3$. The fit (not shown) gave the values $\gamma = 6.01(3)$ mJ/mol K^2 and $\beta = 0.66(1)$ mJ/mol K^4. The lattice part βT^3 was then subtracted from the $C(T)$ data at $H = 0$ to obtain the electronic part of the heat capacity C_{el}. The electronic heat capacity divided by temperature C_{el}/T versus T is shown in Fig. 2(b). An extremely sharp transition at the onset of superconductivity is observed at $T_c = 1.72$ K. The normal state Sommerfeld coefficient $\gamma = 6.01$ mJ/mol K^2 is indicated by an extrapolation [dashed line in Fig. 2(b)] to $T = 0$ of the normal state data. An equal entropy construction (not shown) gave almost the same $T_c = 1.69$ K, indicating no broadening or smearing out of the superconducting transition due to sample inhomogeneities or imperfections.

The data at the lowest temperatures were fit by the expression $C_{\text{el}}/T = \gamma_{\text{res}} + A\exp(-\Delta/T)$, where γ_{res} is the residual Sommerfeld coefficient from the nonsuperconducting fraction of the sample and the second term is a phenomenological exponential decay expected for a gapped (s-wave superconductor) system. The fit shown in Fig. 2(b) as the solid curve through the data below $T = 0.5$ K gave the value $\gamma_{\text{res}} = 0.4$ mJ/mol K^2. With the total $\gamma = 6.01$ mJ/mol K^2, this suggests that ≈7% of the sample volume is nonsuperconducting. An excellent fit of the low temperature C_{el} data to an exponential dependence suggests a conventional s-wave superconducting order parameter.

The magnitude of the anomaly in heat capacity at the superconducting transition is another measure of the nature (weak or strong coupling, single, or multigap) of superconductivity. From the data in Fig. 2(b), we estimate $\Delta C/\gamma T_c \approx 1.52$, which is close to the value 1.43 expected for a conventional, weak-coupling, single-gap BCS superconductor. This further

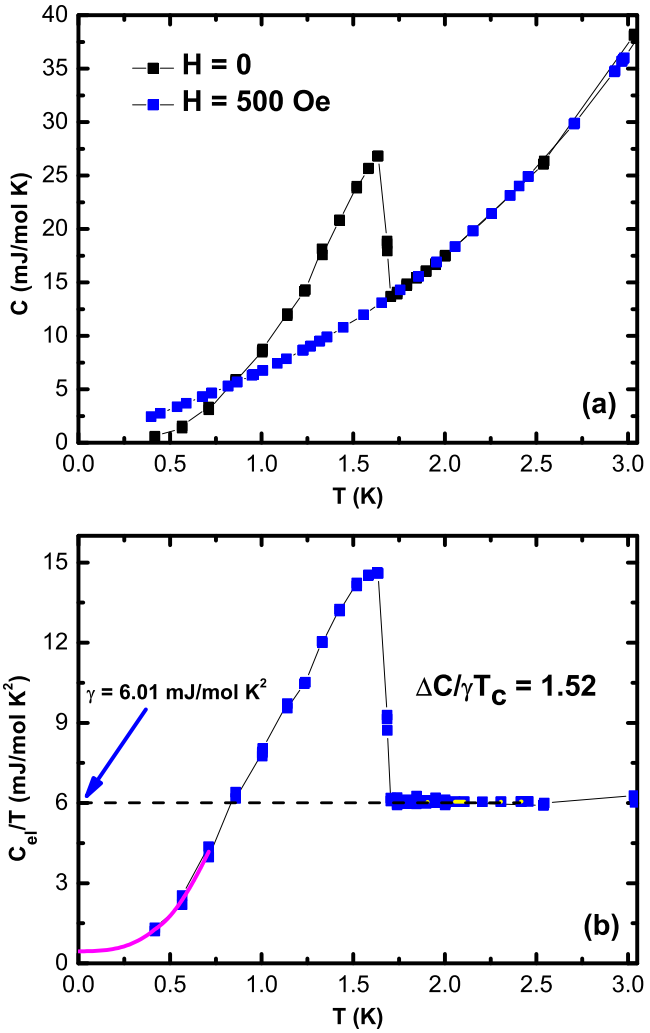

FIG. 2. (a) Heat capacity C versus T for $PdTe_2$ measured in $H = 0$ and $H = 500$ Oe. (b) Electronic contribution to the heat capacity divided by temperature C_{el}/T. The horizontal dash-dot line is the value $\gamma = 6.01$ mJ/mol K^2 and the solid curve through the lowest T data is a fit by a gapped model (see text for details).

supports the conventional nature of superconductivity in $PdTe_2$.

Heat capacity C versus T measurements at various magnetic fields are shown in Fig. 3(a). As expected, the superconducting transition temperature is monotonically suppressed to lower temperatures and its magnitude becomes smaller at higher fields as seen in Fig. 3(a). From an equal entropy construction for the $C(T)$ data at each H, we extract the T_c at that H and use it to draw a critical-field H_c versus temperature ($H_c - T$) phase diagram, which we will discuss later. From the $C(T)$ data at various H, the lattice part was subtracted to get the electronic part $C_{el}(T)$. This data is shown in Fig. 3(b), plotted as C_{el}/T vs T. The data for each H were fit by the expression $C_{el}/T = \gamma_{res} + A\exp(-\Delta/T)$ to get $\gamma_{res}(H)$. For an s-wave superconductor one expects $\gamma_{res}(H) \propto H$. Whereas for a nodal superconductor, $\gamma_{res}(H) \propto H^{1/2}$ is expected, which is called the Volovik effect Ref. [39]. Fig. 3(c) shows that $\gamma_{res}(H)$ follows a linear in H dependence, further supporting conventional superconductivity in $PdTe_2$.

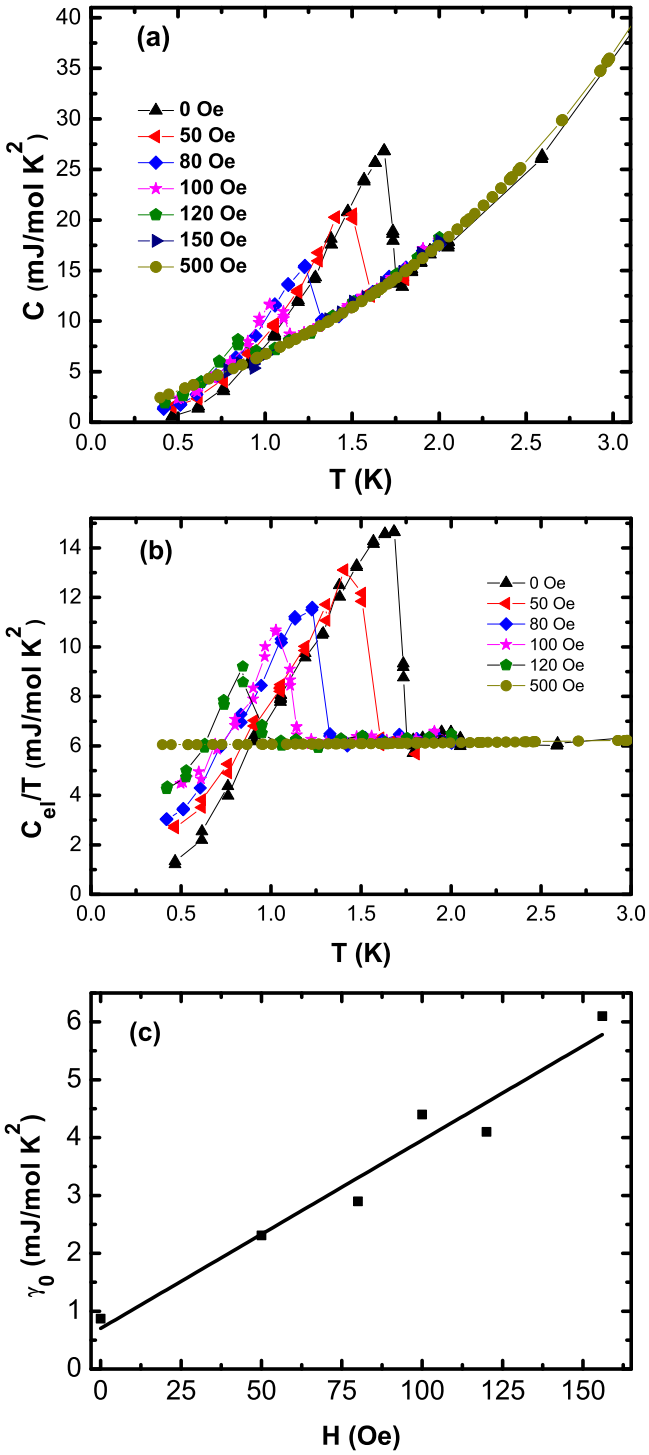

FIG. 3. (a) Heat capacity C versus T for $PdTe_2$ between $T = 0.4$ and 3 K, measured in various magnetic fields H. (b) The electronic contribution to the heat capacity C_{el} divided by T at various H. (c) The $T = 0$ value of the Sommerfeld coefficient $\gamma_0 = C_{el}/T$ vs H. The solid line through the data is a linear fit.

Finally, the $H_c - T$ phase diagram obtained from the $C(T,H)$ data above is shown in Fig. 4 and also follows a conventional behavior expected for a BCS superconductor. In particular, we were able to fit the data with the phenomenological expression $H_c(T) = H_c(0)[1 - (T/T_c)^2]$, with

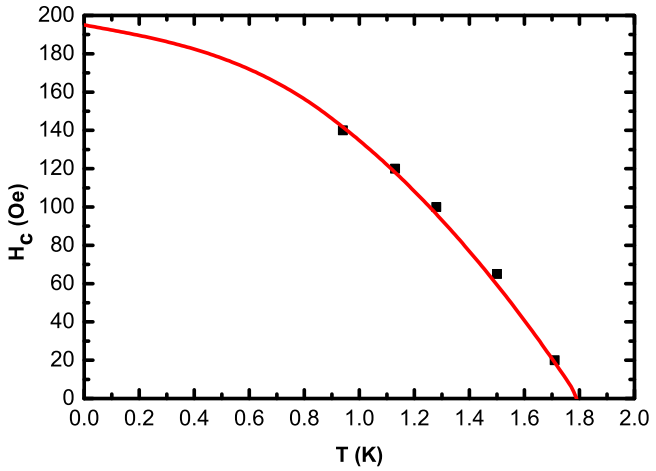

FIG. 4. The critical magnetic field H_c versus temperature T phase diagram extracted from the C versus T data measured at various H shown in Fig. 3. The solid curve through the data is a fit by a phenomenological dependence (see text for details).

the $T = 0$ critical field $H_c(0)$, and the critical temperature T_c as fit parameters. The fit shown as the solid curve through the data in Fig. 4 gave the values $H_c(0) = 195(2)$ Oe and $T_c = 1.78$ K, respectively.

V. SUMMARY AND DISCUSSION

$PdTe_2$ is an interesting material where a superconducting state below $T_c \approx 1.7$ K coexists with a topological band structure. Specifically, $PdTe_2$ has previously been shown to be a type-II Dirac semimetal, raising the possibility of hosting a topological superconducting state. A recent theoretical study of superconductivity in type-II Weyl metals, relevant for $PdTe_2$, predicts a superconducting state with nodes in the gap function [7]. Such a state leads to a $C_{\rm el} \sim T^3$ behavior in the superconducting state in the low temperature limit. This in turn would lead to a reduced jump in the heat capacity at T_c. Nodes in the gap function also lead to the observation of the Volovik effect in a magnetic field, $C_{\rm el}/T \sim \sqrt{H}$ [39].

In this paper, we have used thermodynamic measurements on high quality single crystals of $PdTe_2$ to probe the nature of the superconductivity. Our heat capacity measurements confirm bulk superconductivity at $T_c = 1.7$ K and show that the anomaly at T_c is characterized by the ratio $\Delta C/\gamma T_c \approx 1.5$, which is close to the value 1.43 expected for a weak-coupling, single-band BCS superconductor. The electronic contribution to the heat capacity $C_{\rm el}$ at the lowest temperatures shows an exponential T dependence, which points to a gapped s-wave superconductivity. From H dependent $C(T)$ measurements, we find $C_{\rm el}/T \sim H$, in contrast with behavior expected for nodal superconductivity. Additionally, the critical field versus temperature phase diagram shows a behavior expected for a conventional superconductor. Therefore, all our results strongly indicate that, in spite of the presence of a topological band in the electronic band-structure of $PdTe_2$, which contributes to the transport properties, the superconductivity in $PdTe_2$ is most likely conventional in character.

While there are very few direct predictions of signatures of TSC in heat capacity measurements, most theoretical work on TSC predict unconventional order parameters with point or line nodes in the SC gap structure. Nodes in the gap structure would lead to a nonexponential T dependence of the electronic heat capacity in the SC state as $T \to 0$. There are also predictions of mixed order parameters with an s-wave component plus other unconventional components to the SC gap. In such cases, depending on the fraction of the unconventional component, the heat capacity could be exponential (mostly s-wave component) or might deviate from it. However, because of this extra non-s-wave component, the entropy balance will necessarily lead to the jump in the heat capacity at T_c to become smaller than the BCS value. In our case, the jump is close to and, in fact, slightly larger than the BCS value. Thus, our heat capacity results rule out such scenarios. So, in the least, our results put strong constraints on what kind of TSC, if any at all, could exist in $PdTe_2$.

A recent ac and dc magnetic study on $PdTe_2$ has found a similar $H - T$ phase diagram consistent with conventional bulk superconductivity [37].

ACKNOWLEDGMENT

We thank the x-ray and SEM facilities at IISER Mohali.

[1] M. Sato and Y. Ando, Rep. Prog. Phys. **80**, 076501 (2017).
[2] J. Alicea, Rep. Prog. Phys. **75**, 076501 (2012).
[3] S. R. Elliot and M. Franz, Rev. Mod. Phys. **87**, 137 (2015).
[4] G. Bednik, A. A. Zyuzin, and A. A. Burkov, Phys. Rev. B **92**, 035153 (2015).
[5] S. Kobayashi and M. Sato, Phys. Rev. Lett. **115**, 187001 (2015).
[6] T. Hashimoto, S. Kobayashi, Y. Tanaka, and M. Sato, Phys. Rev. B **94**, 014510 (2016).
[7] M. Alidoust, K. Halterman, and A. A. Zyuzin, Phys. Rev. B **95**, 155124 (2017).
[8] Y. S. Hor, A. J. Williams, J. G. Checkelsky, P. Roushan, J. Seo, Q. Xu, H. W. Zandbergen, A. Yazdani, N. P. Ong, and R. J. Cava, Phys. Rev. Lett. **104**, 057001 (2010).
[9] M. Kriener, K. Segawa, Z. Ren, S. Sasaki, and Y. Ando, Phys. Rev. Lett. **106**, 127004 (2011).
[10] Z. Liu, X. Yao, J. Shao, M. Zuo, L. Pi, S. Tan, C. Zhang, and Y. Zhang, J. Am. Chem. Soc. **137**, 10512 (2015).
[11] T. Asaba, B. J. Lawson, C. Tinsman, L. Chen, P. Corbae, G. Li, Y. Qiu, Y. S. Hor, L. Fu, and L. Li, Phys. Rev. X **7**, 011009 (2017).
[12] Y. S. Hor, J. G. Checkelsky, D. Qu, N. P. Ong, and R. J. Cava, Phys. J. Chem. Solids **72**, 572 (2011).
[13] Amit and Y. Singh, J. Supercond. Novel Mag. **29**, 1975 (2016).
[14] A. S. Erickson, J.-H. Chu, M. F. Toney, T. H. Geballe, and I. R. Fisher, Phys. Rev. B **79**, 024520 (2009)

[15] G. Balakrishnan, L. Bawden, S. Cavendish, and M. R. Lees, Phys. Rev. B **87**, 140507 (2013).
[16] J. L. Zhang, S. J. Zhang, H. M. Weng, W. Zhang, L. X. Yang, Q. Q. Liu, S. M. Feng, X. C. Wang, R. C. Yu, L. Z. Cao, L. Wang, W. G. Yang, H. Z. Liu, W. Y. Zhao, S. C. Zhang, X. Dai, Z. Fang, and C. Q. Jin, Proc. Natl. Acad. Sci. USA **108**, 24 (2010).
[17] G. M. Luke, Y. Fudamoto, K. M. Kojima, M. I. Larkin, J. Merrin, B. Nachumi, Y. J. Uemura, Y. Maeno, Z. Q. Mao, Y. Mori, H. Nakamura, and M. Sigrist, Nature **394**, 558 (1998).
[18] J. D. Sau, R. M. Lutchyn, S. Tewari, and S. Das Sarma, Phys. Rev. Lett. **104**, 040502 (2010).
[19] J. Alicea, Phys. Rev. B **81**, 125318 (2010).
[20] V. S. Pribiag, A. J. A. Beukman, F. Qu, M. C. Cassidy, C. Charpentier, W. Wegscheider, and L. P. Kouwenhoven, Nat. Nanotech. **10**, 593 (2015).
[21] C. Beenakker and L. Kouwenhoven, Nat. Phys. **12**, 618 (2016).
[22] L. Aggarwal, A. Gaurav, G. S. Thakur, Z. Haque, A. K. Ganguli, and G. Sheet, Nat. Mater. **15**, 32 (2015).
[23] H. Wang, H. Wang, H. Liu, H. Lu, W. Yang, S. Jia, X. J. Liu, X. C. Xie, J. Wei, and J. Wang, Nat. Mater. **15**, 38 (2015).
[24] S. Das, L. Aggarwal, S. Roychowdhury, M. Aslam, S. Gayen, K. Biswas, and G. Sheet, Appl. Phys. Lett. **109**, 132601 (2016).
[25] H. Huang, S. Zhou, and W. Duan, Phys. Rev. B **94**, 121117 (2016).
[26] H. J. Noh, J. Jeong, E. J. Cho, K. Kim, B. I. Min, and B.-G. Park, Phys. Rev. Lett. **119**, 016401 (2017).
[27] F. Fei, X. Bo, R. Wang, B. Wu, J. Jiang, D. Fu, M. Gao, H. Zheng, Y. Chen, X. Wang, H. Bu, F. Song, X. Wan, B. Wang, and G. Wang, Phys. Rev. B **96**, 041201 (2017).
[28] M. Yan, H. Huang, K. Zhang, E. Wang, W. Yao, K. Deng, G. Wan, H. Zhang, M. Arita, H. Yang, Z. Sun, H. Yao, Y. Wu, S. Fan, W. Duan, and S. Zhou, Nat. Commun. **8**, 257 (2017).
[29] Y. Xu, F. Zhang, and C. Zhang, Phys. Rev. Lett. **115**, 265304 (2015).
[30] A. A. Soluyanov, D. Gresch, Z. Wang, Q. Wu, M. Troyer, X. Dai, and B. A. Bernevig, Nature **527**, 495 (2015).
[31] H. Weng, C. Fang, Z. Fang, B. A. Bernevig, and X. Dai, Phys. Rev. X **5**, 011029 (2015).
[32] S.-Y. Xu, I. Belopolski, N. Alidoust, M. Neupane, G. Bian, C. Zhang, R. Sankar, G. Chang, Z. Yuan, C.-C. Lee, S.-M. Huang, H. Zheng, J. Ma, D. S. Sanchez, B. Wang, A. Bansil, F. Chou, P. P. Shibayev, H. Lin, S. Jia, and M. Z. Hasan, Science **349**, 613 (2015).
[33] K. Deng, G. Wan, P. Deng, K. Zhang, S. Ding, E. Wang, M. Yan, H. Huang, H. Zhang, Z. Xu, J. Denlinger, A. Fedorov, H. Yang, W. Duan, H. Yao, Y. Wu, S. Fan, H. Zhang, X. Chen, and S. Zhou, Nat. Phys. **12**, 1105 (2016).
[34] L. Huang, T. M. McCormick, M. Ochi, Z. Zhao, M.-T. Suzuki, R. Arita, Y. Wu, D. Mou, H. Cao, J. Yan, N. Trivedi, and A. Kaminski, Nat. Mater. **15**, 1155 (2016).
[35] J. Jiang, Z. K. Liu, Y. Sun, H. F. Yang, C. R. Rajamathi, Y. P. Qi, L. X. Yang, C. Chen, H. Peng, C.-C. Hwang, S. Z. Sun, S.-K. Mo, I. Vobornik, J. Fujii, S. S. P. Parkin, C. Felser, B. H. Yan, and Y. L. Chen, Nat. Commun. **8**, 13973 (2017).
[36] F. Jellinek, Arkiv. Kemi **20**, 447 (1963).
[37] H. Leng, C. Paulsen, Y. K. Huang, and A. de Visser, Phys. Rev. B **96**, 220506 (2017).
[38] S. Das, Amit, A. Sirohi, L. Yadav, S. Gayen, Y. Singh, and G. Sheet, Phys. Rev. B **97**, 014523 (2018).
[39] G. E. Volovik, JETP Lett. **58**, 469 (1993).